HHS Public Access

Author manuscript

Isr J Chem. Author manuscript; available in PMC 2024 February 01.

Published in final edited form as:

Isr J Chem. 2023 February ; 63(1-2): . doi:10.1002/ijch.202200069.

A Fluorescent Unnatural Mannosamine Derivative with Enhanced Emission Upon Complexation with Cucurbit[7]uril

Anna Kataki-Anastasakou[a], **Shang Jia**[a], **Jonathan C. Axtell**[a], **Ellen M. Sletten**[a]

[a]Department of Chemistry and Biochemistry, University of California Los Angeles, 607 Charles E. Young Drive East, Los Angeles, California 90095, USA

Abstract

Metabolic incorporation of unnatural functionality on glycans has allowed chemical biologists to observe and affect cellular processes. Recent work has resulted in glycan-fluorophore structures that allow for direct visualization of glycan-mediated processes, shining light on their role in living systems. This work describes the serendipitous discovery of a small chemical reporter-fluorophore. Investigations into the mechanism of fluorescence arising from (trimethylsilyl)methylglycine appended on mannosamine suggest rigidity and restriction of lone pair geometry contribute to the fluorescent behaviour. In fact, *in situ* cyclization and encapsulation in cucurbit[7]uril enhance fluorescence to levels that can be observed in live cells. While the reported unnatural mannosamine does not traverse the sialic acid biosynthetic pathway, this discovery may lead to small, “turn-on” chemical reporters for incorporation in living systems.

Keywords

mannosamine; fluorescence; cucurbit[7]uril; chemical reporter; metabolic incorporation

1. Introduction

The incorporation of unnatural functionality on the cell surface through metabolic glycoengineering (MGE) has allowed investigations into the role of glycans in cell-cell communication, signaling, viral infectivity and adhesion.[1–4] Given the relative promiscuity of the sialic acid biosynthetic and salvage pathways, seminal MGE reports involved the modification of *N*-acetyl mannosamine and sialic acid by Reutter and co-workers, who found that acylation can drastically alter receptor-ligand interactions in biological systems.[5–7] Following Reutter’s seminal work, multiple functionalities have been incorporated as chemical reporters on glycans (Figure 1A). Bertozzi and coworkers investigated the effects of azides (Az),[8,9] while the Kumar group incorporated fluorine to assess effects on cell adhesion properties and cell surface interactions in mammalian cell lines.[10–12] Yarema and coworkers incorporated thiols and other small chemical reporter groups in a series of investigations on glycans’ roles in living systems.[13,14] These initial works demonstrated the impact of MGE, which has more recently been leveraged for therapeutic applications.[15]

sletten@chem.ucla.edu .

Supporting information for this article is available on the WWW under https://doi.org/10.1002/ijch.202200069

Some examples include mannosamine derivatives containing, alkyl, azido, or phenyl groups, which alter sialylation levels, resulting in changes in signaling of cell surface receptors and/or proteins that can be leveraged for therapeutic development in oncology.[16–20]

While the sialic acid metabolic pathways are promiscuous enough for small, neutral functionality to be incorporated, many larger reporter groups or therapeutics are not tolerated. To overcome these limitations, the Bertozzi Group introduced the bioorthogonal chemical reporter strategy (Figure 1B), a two-step approach involving the incorporation of a chemical reporter, i.e. a small, reactive functional group (such as the azide), followed by a second labeling step using a bioorthogonal chemical reaction (such as strain-promoted azide-alkyne cycloaddition). Using the bioorthogonal chemical reporter strategy, glycans could be directly visualized by microscopy and identified via proteomics. This approach has been widely adopted by the community and has since been applied to a plethora of biomolecules. In certain applications, the bioorthogonal chemical reporter strategy is limited by the secondorder rate constant of the bioorthogonal reaction and/or background reactivity.[21–23] To overcome these limitations, methods that do not rely on covalent chemistries have been pursued. These include metabolic incorporation of guest molecules to be detected through host–guest chemistry, deemed “bioorthogonal complexation,” or direct incorporation of a fluorophore. To date, the bioorthogonal complexation strategy required the incorporation of inert but larger chemical reporters, namely carboranes, as sialic acid derivatives and allowed cell-surface labeling using micromolar concentrations of the host cucurbit[7]uril. [24]

Fluorophores are often large, hydrophobic structures with extended pi systems that can be larger than metabolites themselves. Impressively, direct incorporation of fluorophores has been accomplished by preparing monosaccharides that require only a single modification through a highly promiscuous metabolic pathway. Two recent examples of direct incorporation of chemical reporter-fluorophores have been exhibited by the Vocadlo[25] and the Wu and Traver groups[26] (Figure 1C). The Vocadlo Group designed a membranepermeable activated *N*-acetyl glucosamine (GlcNAc) analog with a 4-chloro-7-nitrobenzofurazan (NBD) chemical reporter, to achieve metabolic labeling of uridine diphosphate-*N*-acetyl-D-glucosamine:polypetidyl transferase (OGT, GT family 41) in live cells. A similar approach of pre-activation to achieve incorporation of large chemical reporter-fluorophores (Cy3 and Cy5) in mammalian cells was used by the Wu and Traver groups.[26] They leveraged the substrate promiscuity of endogenous glycosyltransferases to directly incorporate fluorophore-labeled monosaccharides. This was the first example of direct fluorophore incorporation in cell-surface glycans.

Here, we report our efforts that began as an approach to expand the scope of bioorthogonal complexation, and concluded at the serendipitous discovery of an intrinsically fluorescent mannosamine derivative composed of a small (trimethylsilyl)methylglycine chemical reporter. We hypothesize that fluorescent behavior of this non-standard fluorophore arises via an intramolecular charge transfer mechanism and is enhanced upon cyclization of the mannosamine derivative to a hemiaminal structure. The rigidity arising from the restricted amine lone pair conformation on the hemiaminal increases brightness and allows visualization in live cells at low concentrations. Binding and encapsulation of the

(trimethylsilyl)-methylglycine moiety with cucurbit[7]uril (**CB[7]**) increases rigidity and further enhances the fluorescence intensity. While this mannosamine derivative is trafficked to the lysosome and not incorporated into cell-surface glycans, the results herein lay the groundwork to explore rotationally restricted amines as fluorescent chemical reporters to directly visualize biological function.

2. Results and Discussion

During our work with high-binding bioorthogonal host-guest pairs with **CB[7]**,[24] we searched for small guests that could be incorporated on the cell-surface via MGE. We chose (trimethylsilyl)methyl amine as it is the smallest **CB[7]**-guest with reasonable binding affinity to allow visualization by bioorthogonal complexation.[24,27] In order to conjugate the guest to the 2-position of mannosamine (Man), a (trimethylsilyl)methyl glycine derivative (**2**) was synthesized (Scheme 1) from (trimethylsilyl)-methylglycine methyl ester (**1**).[28] Acid **2** was activated as a pentafluorophenyl (PFP) ester and conjugated to mannosamine to form desired product **3**. Crude **3** was peracetylated and the Boc group deprotected to yield the desired product **4** as the TFA salt.

With **4** prepared, we evaluated its ability to be metabolically incorporated in Jurkat cells. Surprisingly, statistically significant and concentration-dependent (25–500 μM) fluorescence was observed in all Jurkat cells incubated with **4** (Figure 2A, S1). After multiple repetitions of the synthesis, purification and flow cytometry experiments, we concluded that **4** exhibits intrinsic fluorescent behavior. Given that, at equimolar concentrations (50 μM), neither **Ac_4ManNAz** or **Ac_4ManNAc** showed fluorescence properties (Figures 2B, S2), we hypothesized that the intrinsic fluorescence arises from the (trimethylsilyl)methylamine. CHO and HEK cells were also fluorescent upon treatment with **4**, although overall intensities varied by cell type (Figures 2C, S3–S7). The fact that fluorescence was observed in all three channels (FL1-FL3) (Figure S8) was particularly interesting, and pointed to unique fluorescence behavior in biological systems.

At this point, a series of observations suggested that **4** was not being incorporated into cell-surface glycans. These included tolerance of >100 μM **4** but not **Ac_4ManNAz** or **Ac_4ManNAc** (Figure S2); no fluorescence observed on SDS-PAGE analysis of cell lysates; and time-dependent labeling studies showing a peak at 24 hours (Figures S3–S7). We also performed a competition experiment with **Ac_4ManNAc**, which further supported that **4** was not fully traversing the sialic acid biosynthetic pathway (Figures 2D, S9).

To gain a better understanding of the localization and robustness of the fluorescent signal, HEK cells were treated with **4** (500 μM), and imaged via confocal microscopy (Figures 3A–D, S10–13). We observed intracellular labeling with distinct punctate staining (Figure 3A,B). The puncta displayed robust (93%) colocalization with lysotracker red (Figure 3C). The lack of cell-surface fluorescence and weak colocalization (26%) with cell-surface stains further corroborated that **4** is not incorporated into cell-surface glycans (Figure 3D). Nevertheless, these data demonstrate that the fluorescence observed from **4** is robust enough for direct visualization by confocal microscopy.

These results prompted us to explore the fluorescence mechanism of **4**. The absorbance spectrum of **4** in EtOH has λ_{max} =220 nm but a long tail extending above 500 nm (Figure 4A). Similar long absorbance tails have been observed with poly-L-lysine and lysine/glutamate-rich proteins, where they are attributed to charge transfer transitions.[29] We believe a similar mechanism may occur in **4** between the secondary amine-based donor and carbonyl-based acceptor.[30–33] Model studies with an (aminomethyl)ester similar to **1** also suggest this to be the case (Figure S14). When exciting throughout the extended absorption tail, we observed varied emission spectra (Figure 4B), a phenomenon known as excitation-dependent emission, which is caused by the red-edge effect.[34,35] Strong solvent-solute interactions lead to a distribution of sub-states in the excited state. Thus, when exciting at longer λ, a smaller part of the distribution can be excited.[35,36] As a result, excitation at longer wavelengths leads to emission with gradually decreasing intensity.[35,37,38] The excitation-dependent emission explains why we observed fluorescence in all channels on the flow cytometer.

Obtaining a quantum yield is difficult for compounds that display excitation-dependent emission. We chose excitation at λ=365 nm and performed a relative measurement in ethanol compared to anthracene (Φ_F =27%)[39] (Figure S15). We found **4** to be weakly emissive with a Φ_F =0.94%. Note that in water the emission was significantly weaker and unable to be reliably measured. This low Φ_F value made us question whether **4** was the emissive species observed *in cellulo*, and we investigated if an intermediate in the biosynthetic pathway was a brighter fluorophore.

The first step for the conversion of **4** into sialic acid is deacetylation by intracellular esterases. Thus, we subjected **4** to Zemplen deacetylation conditions (Figure 5A), and observed quantitative conversion to hemiaminal **5**. We found **5** to be stable in the hemiaminal form as observed by ^{1}H NMR, where the anomeric and trimethylsilyl group protons are upfield shifted and the methylene protons of the glycine are split (Figure 5A). We characterized the absorbance and emission of **5** and found it had a more pronounced absorbance band from 270–450 nm, with ~40x greater absorption in this region (Figures 5B, C, S16). The increased absorbance may be attributed to structural rigidification facilitating a conformer where charge transfer is favored. Interestingly, Φ_F of **5** was lower than **4** at 0.39% when measured in analogous conditions. Despite the lower Φ_F, the overall brightness (brightness=$\varepsilon_{365} \times \Phi_F$) of **5** was almost 50 times that of **4** (Figure 5D) leading us to believe that the fluorescence visualized *in cellulo* arose from hemiaminal **5**.

Another avenue to restrict conformation is to form a host-guest complex. The initial design of compound **4** was inspired by its ability to form a host–guest complex with **CB[7]** (Figure 5E). Thus, we characterized the absorbance and emission of **4** and **5** in water (500 μM) in the presence and absence of **CB[7]** (500 μM) (Figure 5E). We found that emission was enhanced by 2x in intensity for both **4** and **5** in the presence of **CB[7]**, likely due to the hydrophobic environment of the host cavity (Figure 5F).

Additionally, the absorbance of **4** increased by 2.5x, which we hypothesize to be the result of restricted motion and increased rigidity. We did not see the same increase in absorbance upon complexation of **5** with **CB[7]** (1.14x change, Figure 5G), which is consistent with **5**

already being locked in a conformer with enhanced charge transfer and its rigidity remaining unchanged upon binding (Figure 5F,G). Overall, we found that encapsulation in **CB[7]** can enhance the brightness of the (aminomethyl)ester fluorophores, suggesting an avenue for fluorogenic probe design.

3. Conclusion

In this report, we introduce a small-sized fluorescent mannos-amine derivative that localizes in the lysosome. Despite weak fluorescence in water, we observed excitation-dependent emission by confocal microscopy and flow cytometry in all three channels with strongest intensity at 405 nm and the FL1 channel, respectively. Through *in vitro* and *in cellulo* studies, we believe that cytosolic esterases deacetylate **4**, which results in *in situ* cyclization to hemiaminal **5**. The newly formed piperidine moiety of **5** further rigidifies the structure and results in ~40x greater absorption and 47x increase in brightness. We hypothesize that **5** is the structure we observe in *in cellulo* experiments, since it is stable and its increased brightness explains our ability to observe it even at 25 μM in live cells. Such fluorescent behavior has been observed in restricted protein sheets,[40] aminosilicon-based macromolecules[37,38,41] and oligo-saccharides.[42] However, we find the fluorescent properties of **5** to be especially unique due to the combination of relatively high brightness and small size. The ability to modulate the fluorescence via encapsulation with **CB[7]** provides additional potential for this small, fluorescent group. Further investigation of the intramolecular charge transfer mechanism and structure-property relationship studies could lead to fluorescent functional groups that can undergo robust metabolic incorporation, and even provide opportunities for “turn-on” chemical reporters upon rigid-ification or interaction with hydrophobic pockets.

Supplementary Material

Refer to Web version on PubMed Central for supplementary material.

Acknowledgements

This work was funded by the NIH under award DP2GM13268. NMR data were obtained on instruments funded by NSF MRI CHE-1048804.

Dedicated to Carolyn Bertozzi for her inspiration, brilliance, and advocacy; and to 2022, the year the world got to realize how amazing Carolyn Bertozzi is.

Data Availability Statement

The data that support the findings of this study are available in the supplementary material of this article.

References

[1]. Bertozzi CR, Acc. Chem. Res 2011, 44, 651–653. [PubMed: 21928847]

[2]. Agatemor C, Buettner MJ, Ariss R, Muthiah K, Saeui CT, Yarema KJ, Nat. Chem. Rev 2019, 3, 605–620.

[3]. Stone SE, Glenn WS, Hamblin GD, Tirrell D, Curr. Opin. Chem. Biol 2017, 36, 50–57. [PubMed: 28088696]

[4]. Liu CC, Jewett MC, Chin JW, Voigt CA, Nat. Chem. Biol 2018, 14, 103–106. [PubMed: 29337969]

[5]. Herrmann M, von der Lieth CW, Stehling P, Reutter W, Pawlita M, J. Virol 1997, 71, 5922–5931. [PubMed: 9223482]

[6]. Keppler OT, Stehling P, Herrmann M, Kayser H, Grunow D, Reutter W, Pawlita M, J. Biol. Chem 1995, 270, 1308–1314. [PubMed: 7836396]

[7]. Keppler OT, Hinderlich S, Langner J, Schwartz-Albiez R, Reutter W, Pawlita M, Science 1999, 284, 1372–1376. [PubMed: 10334995]

[8]. Luchansky SJ, Bertozzi CR, ChemBioChem 2004, 5, 1706–1709. [PubMed: 15568180]

[9]. Prescher JA, Dube DH, Bertozzi CR, Nature 2004, 430, 873–877. [PubMed: 15318217]

[10]. Dafik L, d'Alarcao M, Kumar K, J. Med. Chem 2010, 53, 4277–4284. [PubMed: 20438083]

[11]. Dafik L, d'Alarcao M, Kumar K, Bioorg. Med. Chem. Lett 2008, 18, 5945–5947. [PubMed: 18819798]

[12]. Zamora CY, d'Alarcao M, Kumar K, Bioorg. Med. Chem. Lett 2013, 23, 3406–3410. [PubMed: 23639536]

[13]. Sampathkumar S-G, Li A, Jones MB, Sun Z, Yarema KJ, Nat. Chem. Biol 2006, 2, 149–152. [PubMed: 16474386]

[14]. Mathew MP, Tan E, Saeui CT, Bovonratwet P, Sklar S, Bhattacharya R, Yarema KJ, Oncotarget 2016, 7, 66491–66511. [PubMed: 27613843]

[15]. Dube DH, Bertozzi CR, Nat. Rev. Drug Discovery 2005, 4, 477–488. [PubMed: 15931257]

[16]. Almaraz RT, Tian Y, Bhattarcharya R, Tan E, Chen S-H,Dallas MR, Chen L, Zhang Z, Zhang H, Konstantopoulos K, Yarema KJ, Mol. Cell. Proteomics 2012, 11, M112.017558.

[17]. Tian Y, Almaraz RT, Choi CH, Li QK, Saeui C, Li D, Shah P, Bhattacharya R, Yarema KJ, Zhang H, Clin. Proteomics 2015, 12, 11. [PubMed: 25987888]

[18]. Badr HA, AlSadek DMM, El-Houseini ME, Saeui CT, Mathew MP, Yarema KJ, Ahmed H, Biomaterials 2017, 116, 158–173. [PubMed: 27926828]

[19]. Chefalo P, Pan Y, Nagy N, Harding C, Guo Z, Glycoconjugate J. 2003, 20, 407–414.

[20]. Pan Y, Chefalo P, Nagy N, Harding C, Guo Z, J. Med. Chem 2005, 48, 875–883. [PubMed: 15689172]

[21]. Rossin R, Robillard MS, Curr. Opin. Chem. Biol 2014, 21, 161–169. [PubMed: 25159021]

[22]. Chang PV, Prescher JA, Sletten EM, Baskin JM, Miller IA, Agard NJ, Lo A, Bertozzi CR, Proc. Natl. Acad. Sci. USA 2010, 107, 1821–1826. [PubMed: 20080615]

[23]. Vugts DJ, et al. Bioconjugate Chem. 2011, 22, 2072–2081.

[24]. Kataki-Anastasakou A, Hernandez S, Sletten EM, ACS Chem. Biol 2021, 16, 2124–2129. [PubMed: 34669367]

[25]. Tan HY, Eskandari R, Shen D, Zhu Y, Liu T-W, Willems LI, Alteen MG, Madden Z, Vocadlo DJ, J. Am. Chem. Soc 2018, 140, 15300–15308. [PubMed: 30296064]

[26]. Hong S, Sahai-Hernandez P, Chapla DG, Moremen KW, Traver D, Wu P, Angew. Chem. Int. Ed 2019, 58, 14327–14333; Angew. Chem. 2019, 131, 14465–14471.

[27]. Liu S, Ruspic C, Mukhopadhyay P, Chakrabarti S, Zavalij PY, Isaacs L, J. Am. Chem. Soc 2005, 127, 15959–15967. [PubMed: 16277540]

[28]. Badir SO, Sim J, Billings K, Csakai A, Zhang X, Dong W, Molander GA, Org. Lett 2020, 22, 1046–1051. [PubMed: 31940210]

[29]. Prasad S, Mandal I, Singh S, Paul A, Mandal B, Venkatramani R, Swaminathan R, Chem. Sci 2017, 8, 5416–5433. [PubMed: 28970921]

[30]. Chen YA, et al. Chem. Eur. J 2016, 22, 14688–14695. [PubMed: 27539818]

[31]. Zhang C, et al. Org. Electron 2017, 45, 190–197.

[32]. Tabuchi A, Hayakawa T, Kuwata S, Ishige R, Ando S, Mater. Adv 2021, 2, 5629–5638.

[33]. Meng X, Song L, Zhao J, Han H, Zheng D, J. Phys. Org. Chem 2022, 35, e4320.

[34]. Demchenko AP, Luminescence 2002, 17, 19–42. [PubMed: 11816059]

[35]. Khan S, Gupta A, Verma NC, Nandi CK, Nano Lett. 2015, 15, 8300–8305. [PubMed: 26566016]

[36]. Hongmin Chen, Zipeng Zhen, Wei Tang, Trever Todd, Yen-Jun Chuang, Lianchun Wang, Zhengwei Pan, Jin X, Theranostics 2013, 3, 650–657. [PubMed: 24052805]

[37]. Sá Ferreira RA, Ferreira AL, Carlos LD, Eur. Phys. J. B 2006, 50, 371–378.

[38]. Carlos LD, Ferreira RAS, Pereira RN, Assunção M, Bermudez V. de Z., J. Phys. Chem. B 2004, 108, 14924–14932.

[39]. Dawson WR, Windsor MW, J. Phys. Chem 1968, 72, 3251–3260.

[40]. Pinotsi D, Grisanti L, Mahou P, Gebauer R, Kaminski CF, Hassanali A, Kaminski Schierle GS, J. Am. Chem. Soc 2016, 138, 3046–3057. [PubMed: 26824778]

[41]. Brites CDS, Freitas VT, Ferreira RAS, Millán A, Palacio F, Carlos LD, Langmuir 2012, 28, 8190–8196. [PubMed: 22554306]

[42]. Yu Y, Gim S, Kim D, Arnon ZA, Gazit E, Seeberger PH, Delbianco M, J. Am. Chem. Soc 2019, 141, 4833–4838. [PubMed: 30829477]

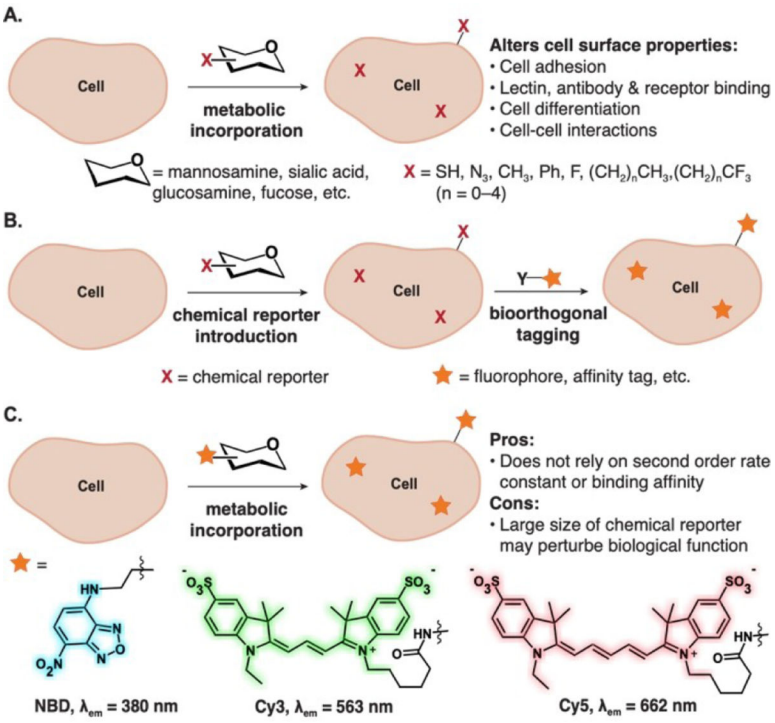

Figure 1.

Applications of metabolic glycoengineering. (**A**) Metabolic glycoengineering to introduce small, unnatural functionality (i.e. “chemical reporter”) *in vivo* alters cell surface properties. (**B**) (**i**) Bioorthogonal tagging of cell surface glycans relies on incorporation of chemical reporters followed by a selective chemical reaction or strong non-covalent interaction. (**C**) Metabolic incorporation of large fluorophores through MGE results in direct visualization of glycans in living systems.

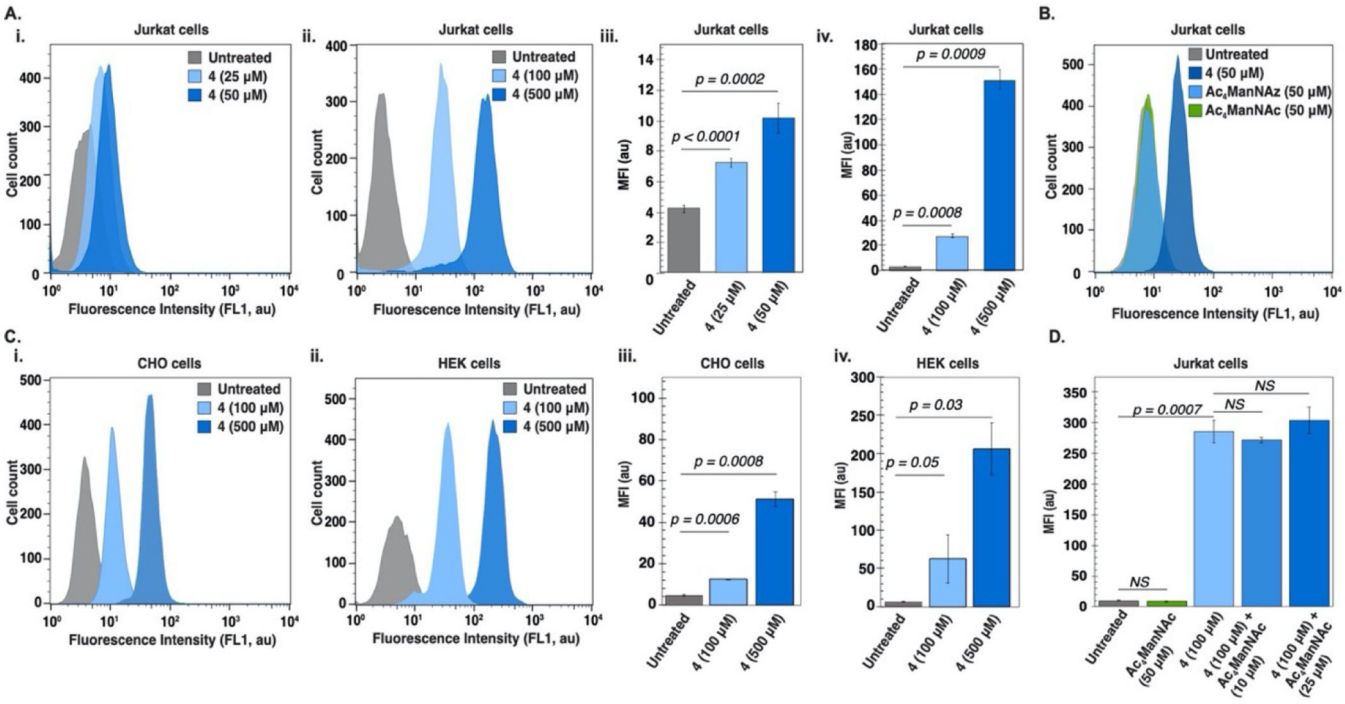

Figure 2.

Flow cytometry of cells treated with **4** indicates **4** is fluorescent. (**A**) Jurkat cells grown in the presence or absence of **4** at 37°C, 5% CO_2 for three days. (**i, ii**) Histograms of a single replicate exhibiting **4** (25–50 μM) and **4** (100–500 μM) fluorescence, respectively and (**iii**, **iv**) analysis of triplicate experiments. (**B**) Peracetylated mannosamine compounds (**4, Ac_4ManNAz, Ac_4ManNAc**) used in a comparison experiment of intrinsic fluorescent properties after incubation at 37°C, 5% CO_2 for three days. (**C**) Histograms representing fluorescence from a single replicate of HEK (**i**) or CHO (**ii**) cells treated with **4** (0–50 μM) at 37°C, 5% CO_2 for three days; (**iii**, **iv**) respective analysis of triplicate experiments. (**D**) Competition experiment of Jurkat cells incubated with **4** (100 μM) in the presence of increasing concentrations of **Ac_4ManNAc** (0–25 μM) at 37°C, 5% CO_2 for three days. Error bars represent the standard deviation of triplicate experiments. For statistical analysis, a one-tailed Student's t-test was used and statistical significance was set at $p<0.05$.

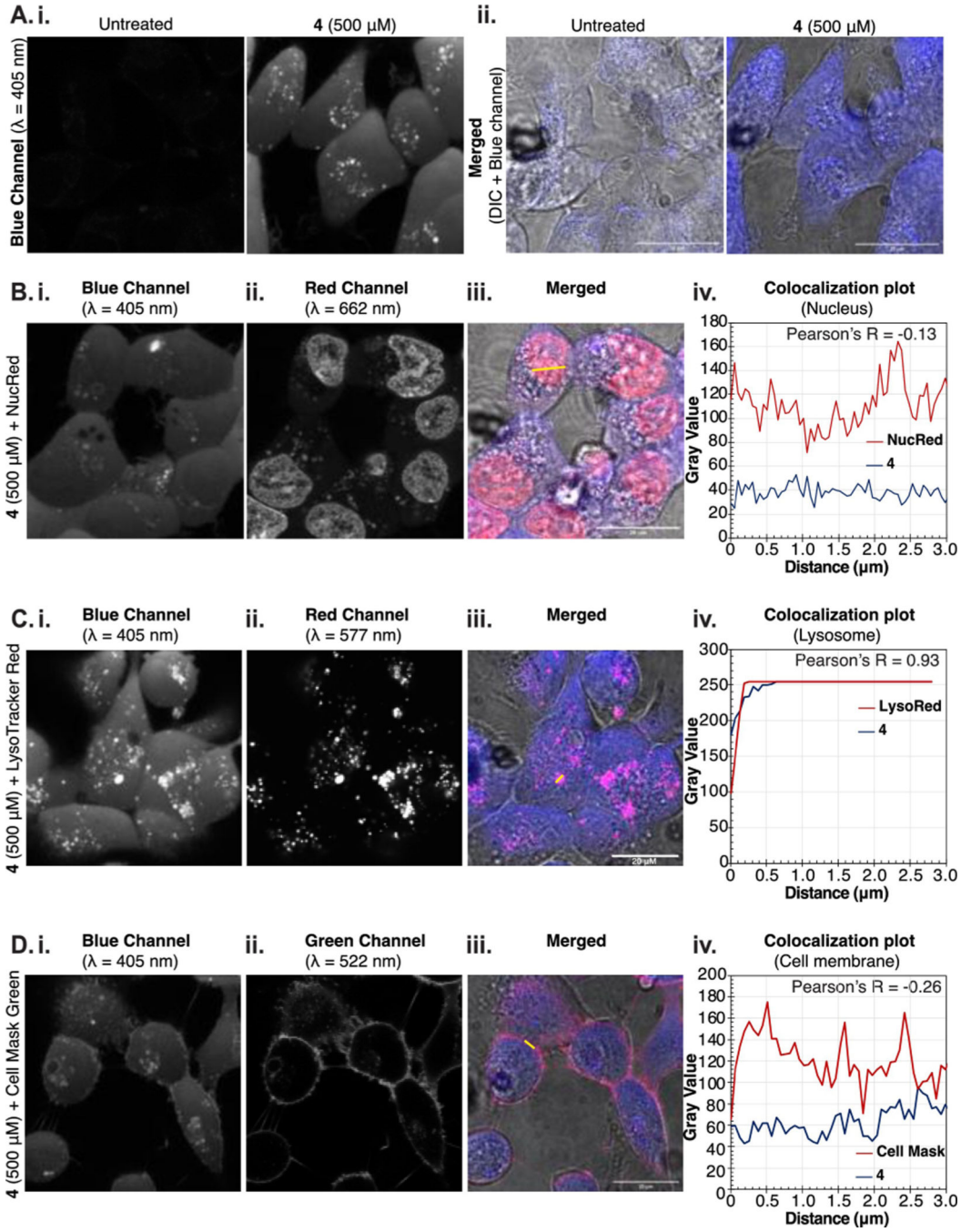

Figure 3.

Microscopy of HEK cells treated with **4. (A)** HEK cells were incubated with/out **4** (500 μM) for 24 h at 37°C, 5% CO_2 and imaged by confocal microscopy; (i) single channel images (λ= 405 nm); (ii) overlay with differential interference contrast. (**B-D**) Localization of **4** was studied by co-staining with NucRed Live 647 (B), LysoTracker Red DN-99 (C) and Cell Mask Green (D) and imaged by confocal microscopy. (i) Blue channel visualizing **4** (λ= 405 nm); (ii) Red (λ=662 nm (B), 577 nm (C) or green (λ=522 nm) channels for organelle staining; (**iii**) merged images of **4** (blue), organelle stain (pink) and DIC; (**iv**)

Pearson correlation plots to indicate the colocalization of **4** (blue line) with the nucleus (B), lysosome (C), or cell membrane (D) (red line) based on cross section shown as yellow line in (iii).

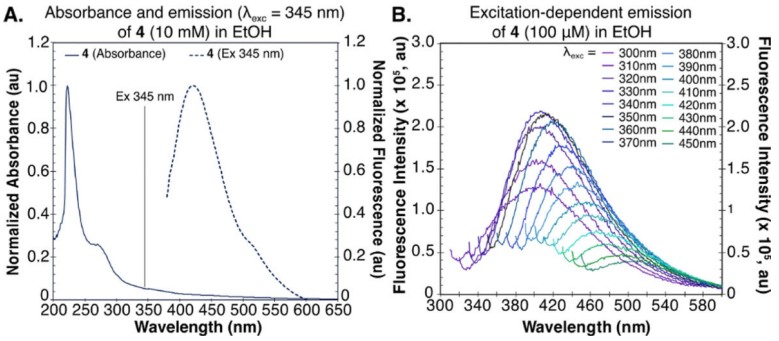

Figure 4.

Photophysical properties of **4**. (**A**) Absorption and emission spectra of **4** (10 mM) in EtOH. **(B**) Excitation-dependent emission of **4** (10 mM in EtOH) in a range of excitation wavelengths (λ_{exc}=300–450 nm).

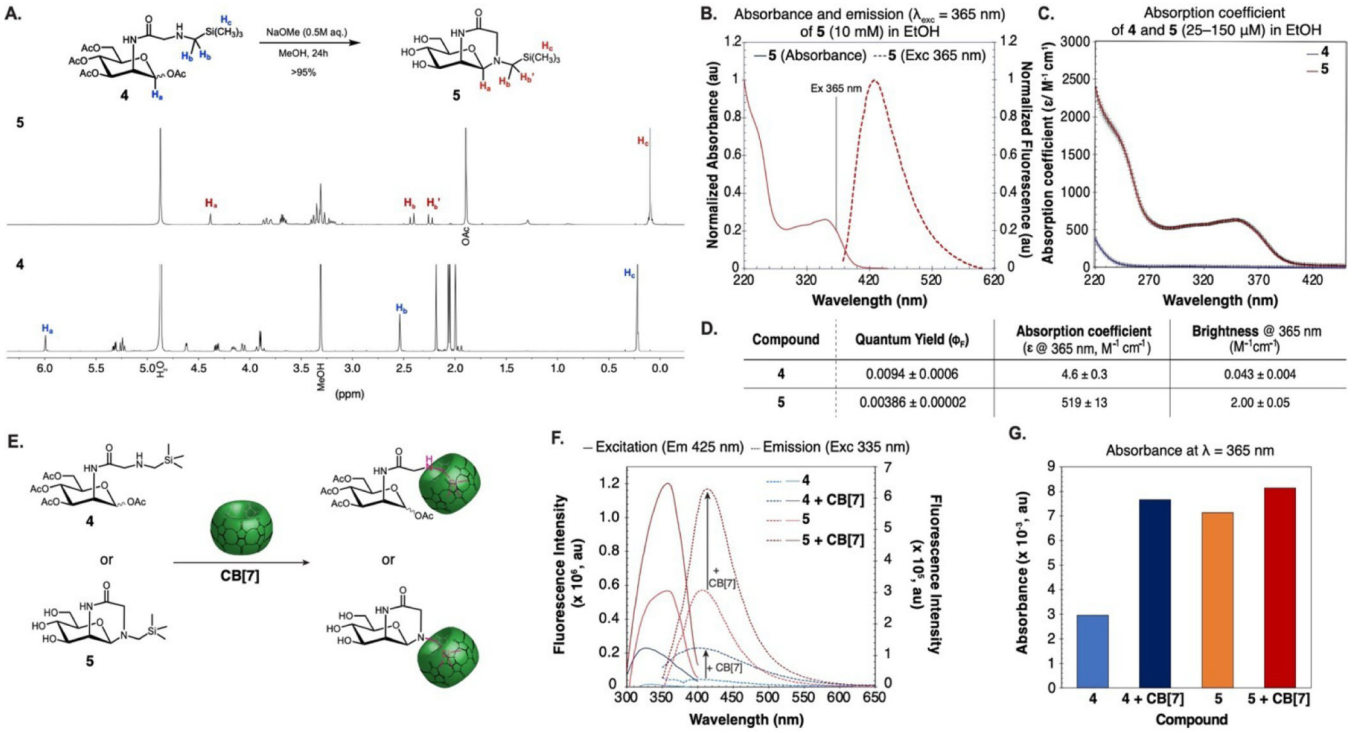

Figure 5.

Brightness of **4** is enhanced by cyclization and/or encapsulation with **CB[7]**. (**A**) ^{1}H NMR of **4** before and after deacetylation. No purification was performed before the ^{1}H NMR of **5** was obtained. (**B**) Absorption and emission spectra of **5** (10 mM) in EtOH. (**C**) Absorption coefficient of **4** and **5** at λ=220–450 nm. (**D**) Table of photophysical properties of **4** and **5**. (**E**) Schematic depicting the complexation of **CB[7]** with **4** and **5** to increase fluorescence intensity. (**F**) Comparison of emissive properties: excitation spectra with emission at 425 nm and emission spectra with excitation at 335 nm of **4** (500 μM) and **5** (500 μM) in the presence or absence of **CB[7]** (500 μM) in H_2O. (**G**) Absorbance at λ=365 nm of **4** (500 μM) and **5** (500 μM) in the presence or absence of **CB[7]** (500 μM) in H_2O.

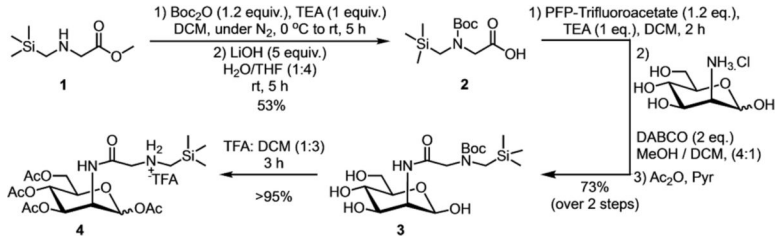

Scheme 1.

Synthesis of peracetylated unnatural mannosamine derivative, **4**.